6A.5 ASSIMILATION OF NON-LOCAL RADIO OCCULTATION MEASUREMENTS AND ITS IMPACT ON WRF MODEL PREDICTION OF HURRICANE EARL IN 2010

Xue Meng Chen[1*], S. H. Chen[1], S. Y. Chen[2], and C. Y. Huang[3]
[1]University of California, Davis, Davis, CA
[2]National Center for Atmospheric Research, Boulder, CO
[3]National Central University, Jhongli, Taoyuan, Taiwan

1. INTRODUCTION

Space-borne Global Positioning System (GPS) Radio Occultation (RO) measurements have the advantage of not being sensitive to weather and offer a global spatial coverage and a high vertical resolution up to three meters. Since the early 20th century, the assimilation of these measurements has improved global and regional predictions, and is actively used in operational weather predictions. Healy et al. (2005) showed that Numerical Weather Prediction analyses and up to four-day forecasts of temperature in upper troposphere and lower stratosphere are significantly improved when retrieved RO refractivity profiles are assimilated, especially in the Southern Hemisphere where other datasets are scarce. Similar results were found by Zou et al. (2004), who also noted a negative bias in refractivity retrievals in the lower troposphere. Hurricane case studies have shown that the use of these observations clearly brings improvement to hurricane predictions (Chen et al. 2009, Liu et al. 2012, Huang et al. 2005).

In Chen et al. (2009), a non-local excess phase observation operator was developed in the Weather Research and Forecasting (WRF) data assimilation (DA) system. Excess phase is the integrated refractivity along a ray path, and was found to have a smaller representativeness error than local refractivity (Sokolovski et al. 2005, Syndergaard et al. 2005). In this study, we look at the impact of assimilating non-local excess phase on the prediction of Hurricane Earl in 2010, and the effect of tripling the vertical resolution of data assimilated by increasing vertical levels during data assimilation. Assimilation of more data points better represents the highly variable thermodynamic fields in a tropical cyclone environment, and increases the impact of RO observations on model simulations.

* *Corresponding author address:* Xue Meng Chen, Univ. of California, Davis, Dept. of Land, Air and Water Resources, Davis, CA 95616; e-mail: xuechen@ucdavis.edu

2. NUMERICAL EXPERIMENT SETTING

The Weather Research and Forecasting (WRF) model Version 3.2 (Skamarock et al. 2008) and its data assimilation (WRFDA) system (Barker et al. 2004, Barker et al. 2012) were used for the simulations of Hurricane Earl (2010). The assimilation of RO excess phase was implemented into this version of data assimilation. Four numerical experiments were conducted and are summarized in Table 1. During data assimilation, a domain-specific background error covariance is used and calculated following the National Meteorological Center (NMC) method (Parrish and Derber, 1992).

Figure 1 shows a map of all observations used during data assimilation for the different simulations. The control simulation (CTRL) has assimilation of conventional surface and upper-level sounding observations from the Global Telecommunication System (GTS), representing a reference model prediction of the hurricane. The other three experiments have assimilation of both conventional and space-borne GPSRO excess phase observations. The GTS+GPS column (GPGC) experiment has excess phase profiles assimilated as column data. The GPG experiment assimilates each excess phase data point at their actual measured positions (i.e., considering the drifting of perigee points) and thinned to one point per model level. In the GPGD experiment, additional levels are introduced during data assimilation when the RO data points drift across more than one horizontal model grid within one model level. We will call these added levels pseudo model levels, onto which model variables are interpolated to perform data assimilation. As a consequence, excess phase data are assimilated at a higher vertical resolution in GPGD, with an increase in number of between double and triple of the GPG experiment. A schematic representation of the algorithm is shown in Figure 2. The addition of pseudo model levels takes better advantage of the original high vertical resolution of the RO observations, and is expected to give an impact that is the most representative of the dataset.

Initial and boundary conditions of the simulations are provided by the European Center for Medium range Weather Forecasting (ECMWF) Interim reanalysis. All simulations share the same model configuration: Three domains of 27 km, 9 km and 3km horizontal resolutions for domains 1-3, respectively, and 45 vertical levels. Model top extends up to 5000 Pa. The nested domains have two-way interaction with their parent domains, and are moving with the cyclone during the forecast. The physics schemes used are Morrison microphysics scheme (Morrison et al. 2009), YonSei University (YSU) planetary boundary layer scheme (Hong et al. 2006), Kain-Fritsch (KF) cumulus parameterization (Kain 2004) that is deactivated in domain 3 due to its high spatial resolution, Rapid Radiative Transfer Model (RRTM) longwave radiation parameterization (Mlawer et al. 1997), and Goddard shortwave radiation parameterization (Chou and Suarez 1994).

3. RESULTS AND DISCUSSION

From comparison with a test simulation where no observations were used, the main impact from assimilation of GTS observations in the CTRL simulation is an increase in surface pressure north of Hurricane Earl towards the end of data assimilation period, where the subtropical ridge is in place, which likely kept the developing cyclone moving further north, and improved its track. Based on Remote Sensing Systems satellite retrievals of Total Precipitable Water (TPW), the simulation has higher water vapor content within 200km radius of the developing cyclone center throughout the entire data assimilation period. Dee et al. (2011) found a dry bias of about 1kgm^{-2} in a general assessment of the EC-Interim reanalysis for total column water vapor over the tropical North Atlantic region, based on satellite retrievals. In this particular case however, comparison with the same satellite retrievals shows a slightly higher TPW from the reanalysis, which most likely influenced all simulations as the reanalysis was used as the background model state. The higher column water vapor content, and a stronger initial vortex based on EC-Interim reanalysis, might explain the earlier rapid intensification of the CTRL simulation compared to observations as shown in Figure 4.

Excess phase (EPH) delay, through its relationship with air density and the dipole moment of water vapor molecules, directly impacts three model variables: total air pressure, temperature and water vapor mixing ratio. It may also indirectly impact the wind field through the multivariate adjustment and penalty (i.e., the balance equation) in WRFDA. Figure 3 shows the increments, defined as the difference between analysis (after assimilation) and background (before data assimilation), in water vapor mixing ratio (QV) at approximately 5 km, and a vertical cross section of temperature (T) increments, after the assimilation of two EPH profiles that extend into the cyclone region at 1500 UTC on August 26th, encircled in Figure 1. From comparison of QV increments between the GPGC experiment, where positional change of RO observations (i.e., of perigee points) within profiles is ignored, and the GPG experiment, where the observations are assimilated at their correct position, we can see drastic changes in the position of maximum impact regions. Nevertheless, in all three experiments, the resulting increments in QV at that time are mostly negative in the vicinity of the storm, and positive south of the storm, indicating a consistency in the information carried by the excess phase observations. Increments in temperature are exactly the opposite of QV increments, as expected from the inverse relationship of T with refractivity and water vapor content.

Higher spatial variability is resolved in the GPGD experiment as shown in the vertical cross-section of the temperature increments field. The addition of data points assimilated also increased the magnitude of increments, around 0.6 K in temperature as seen in Fig. 2, and 0.2 g/kg in QV.

The use of excess phase observations, independent of the way they were assimilated, resulted in a higher TPW and a higher near-surface relative vorticity in the vicinity of the cyclone during the data assimilation period, compared to assimilation of only GTS observations (CTRL), which is also reflected in an earlier deepening of the central pressure minimum, closer to observations. Considering the fact that the CTRL simulation started with a weaker cyclone than the other experiments, the GPGD experiment seems to have better captured the initial state of the cyclone that lead to the period of rapid intensification.

4. REFERENCES

Barker, D., W. Huang, Y. R. Guo, and A.Bourgeois, 2003: A three-dimensional variational (3DVAR) data assimilation system for use with MM5. NCAR Technical Note NCAR/TN-453+STR, 68 pp.

Barker, D., W. Huang, Y. R. Guo, A. J. Bourgeois, and Q.N. Xiao, 2004: A three-dimensional variational data assimilation sys tem for MM5: Implementation and initial results. *Mon. Wea. Rev.*, **132**, 897-914

Chen, S.-Y., C.-Y. Huang, Y.-H. Kuo, Y.-R. Guo, and S. Sokolovskiy, 2009: Assimilation of GPS Refractivity from FORMOSAT-3/COSMIC Using a Nonlocal Operator with WRF 3DVAR and Its Impact on the Prediction of a Typhoon Event. *Terr. Atmos. Ocean. Sci.*, **20**, 133-154.

Chou, M.-D., M. J. Suarez, X.-Z. Liang, and M. M.-H. Yan, 2001: A thermal infrared radiation parameterization for Atmospheric Studies. *NASA Tech. Memo.*, 104606, **19**, 102 pp.

Dee, D.P. et al., 2011: The ERA-Interim reanalysis: configuration and performance of the data assimilation system. *Q.J.R.Meteorol.Soc.*, **137**, 553-597.

Healy, S.B., A.M. Jupp, and C. Marquardt, 2005: Forecast impact experiment with GPS radio occultation measurements. *Geophys. Res. Lett.*, **32**, L03804, doi:10.1029/2004GL020806.

Hong, Song–You, Yign Noh, Jimy Dudhia, 2006: A new vertical diffusion package with an explicit treatment of entrainment processes. *Mon. Wea. Rev.*, **134**, 2318–2341.

Huang, C.-Y., Y.-H. Kuo, S.-H. Chen, and F. Vandenberghe, 2005: Improvements in Typhoon Forecasts with Assimilated GPS Occultation Refractivity. *Wea. Forecasting, AMS,* **20**, 931-953.

Kain, John S., 2004: The Kain–Fritsch convective parameterization: An update. *J. Appl. Meteor.*, **43**, 170–181.

Liu, H., J. Anderson, Y.-H. Kuo, 2012: Improved Analyses and Forecasts of Hurricane Ernesto's Genesis Using Radio Occultation Data in an Ensemble Filter Assimilation System. *Mon. Wea. Rev.*, **140**, 151–166.

Mlawer, Eli. J., Steven. J. Taubman, Patrick. D. Brown, M. J. Iacono, and S. A. Clough (1997), Radiative transfer for inhomogeneous atmospheres: RRTM, a validated correlated–k model for the longwave. *J. Geophys. Res.*, **102**, 16663–16682.

Morrison, H., G. Thompson, V. Tatarskii, 2009: Impact of Cloud Microphysics on the Development of Trailing Stratiform Precipitation in a Simulated Squall Line: Comparison of One– and Two–Moment Schemes. *Mon. Wea. Rev.*, **137**, 991–1007.

Parrish, D.F. and J.C. Derber, 1992: The National Meteorological Center's Spectral Statistical-Interpolation Analysis System. *Mon. Wea. Rev., AMS*, **120**, 1747-1763.

Skamarock, W.C. et al., 2008: A Description of the Advanced Research WRF Version 3. NCAR technical note NCAR/TN-475+STR, 113 pp.

Sokolovskiy, S., Y.-H. Kuo, and W. Wang, 2005: Assessing the Accuracy of a Linearized Observation Operator for Assimilation of Radio Occultation Data: Case Simulations with a High-Resolution Weather Model. *Mon. Wea. Rev., AMS*, **133**, 2200-2212.

Syndergaard, S., E.R. Kursinski, B.M. Herman, E.M. Lane, and D.E. Flittner, 2005: A Refractive Index Mapping Operator for Assimilation of Occultation Data. *Mon. Wea. Rev., AMS*, **133**, 2650-2668.

Zou, X., H. Liu, R.A. Anthes, H. Shao, J.C. Chang, and Y.-J. Zhu, 2004: Impact of CHAMP Radio Occultation Observations on Global Analysis and Forecasts in the Absence of AMSU Radiance Data. . *J. Meteorol. Soc. Jpn.*, **82**, No. 1B, 533–549.

5. TABLES AND FIGURES

Table 1 Numerical simulations of Hurricane Earl 2010.

Experiments	Observations assimilated
CTRL	GTS
GPGC	GTS + GPS RO column, thinned to model vertical resolution
GPG	Same as GPGC, except considering the horizontal drifting of perigee points
GPGD	Same as GPG, except more data assimilated with the addition of pseudo model levels

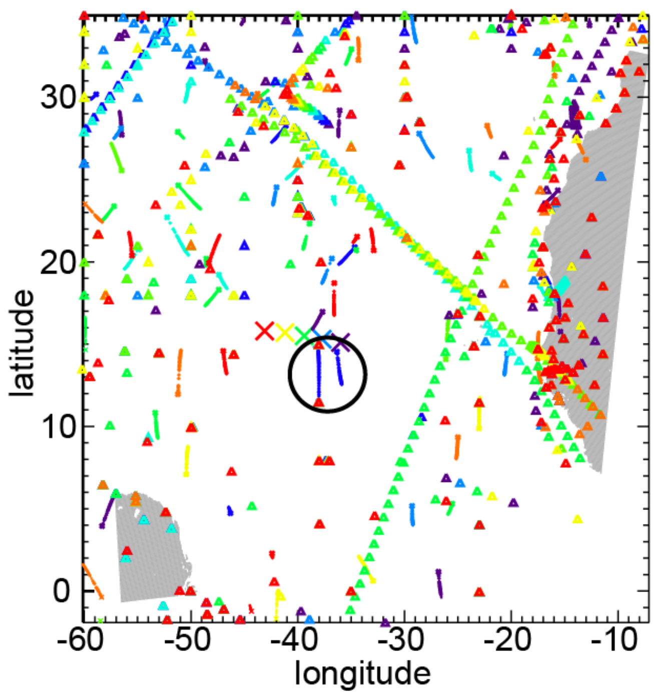

Figure 1 Map of all assimilated observations in domain 2, color indicating the time of assimilation, from 1200 UTC August 26th in purple, to 1200 UTC August 27th in red. GTS surface and upper-air soundings are symbolized by triangles, GPS RO profiles are lines formed by horizontally drifting perigee points. Crosses indicate the positions of the observed cyclone as reported by the National Hurricane Center. Two radio occultation profiles that were measured within the storm area and that likely impacted the simulations are encircled.

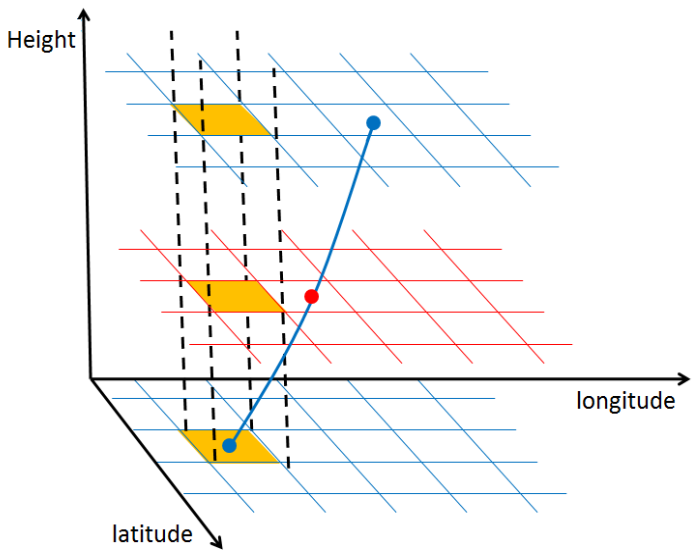

Figure 2 Schematic diagram of adding a pseudo level (in red) into existing model levels (in blue), when radio occultation perigee points drift horizontally across more than one model grid between model vertical levels.

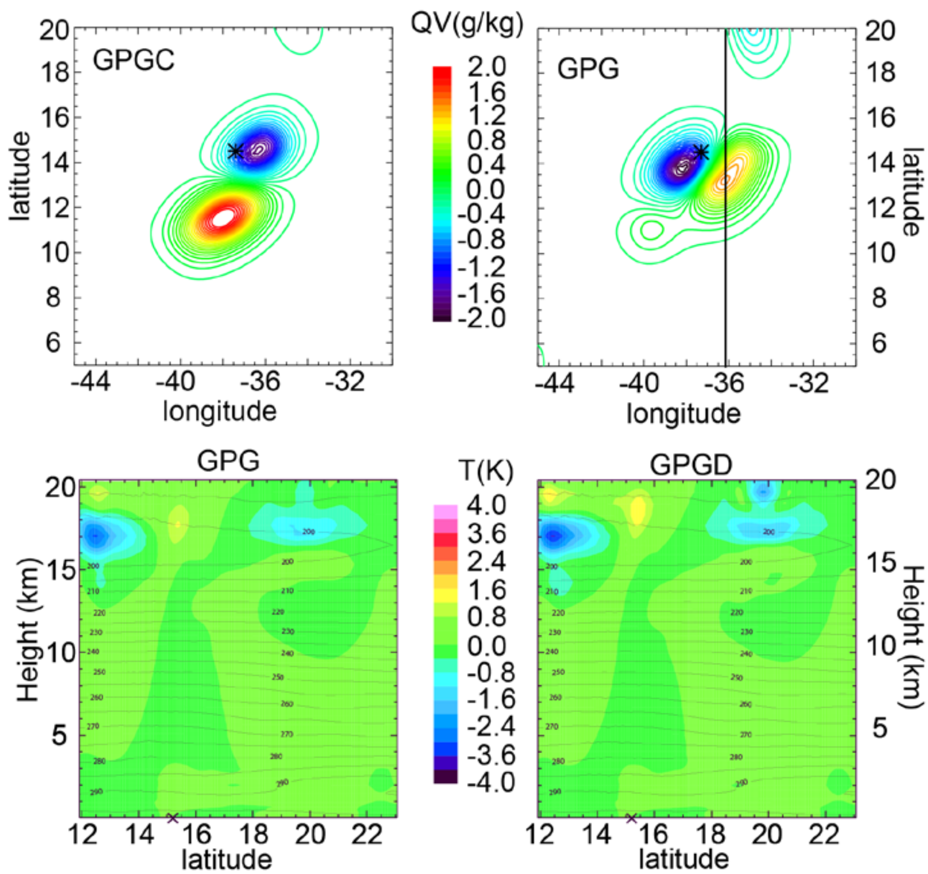

Figure 3 Horizontal cross-section of the 17th model level (~5km height) of the water vapor mixing ratio (QV) increments from the GPGC and GPG simulations, and vertical cross-section of the temperature (T) increments from the GPG and GPGD simulations along the line at -36.2º west as shown in the top-right QV increment. These increments result from the assimilation of the two RO profile encircled in Figure 1, at 1500UTC on 26th August 2010. Crosses indicate the position of the simulated cyclones.

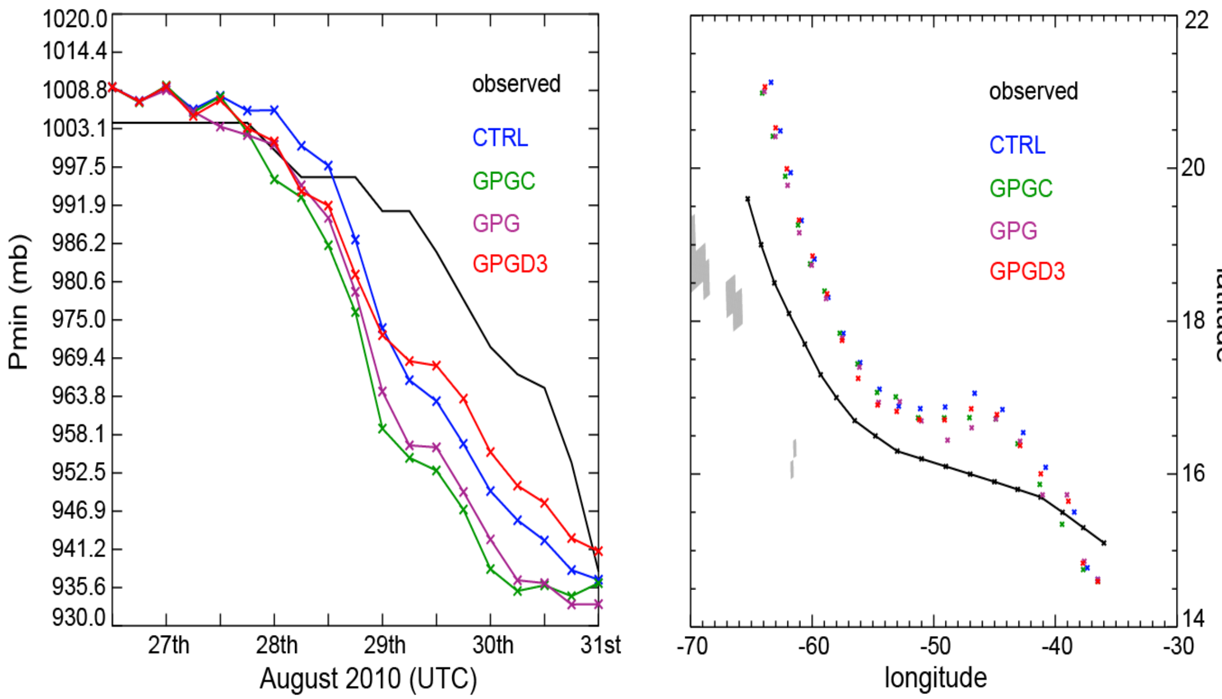

Figure 4 Central minimum sea level pressure and track of the simulated cyclones, compared to the reported values by the National Hurricane Center (observed).